REDUCED ORDER MODEL OF GLASS PLATE LOADED BY LOW-VELOCITY IMPACT

TOMÁŠ JANDA, ALENA ZEMANOVÁ, PETR HÁLA, PETR KONRÁD &
JAROSLAV SCHMIDT
Czech Technical University in Prague, Czech Republic.

ABSTRACT
This article concerns a reduced order model of unconstrained glass plate exposed to low-velocity impact. First, three-parametric model consisting of two masses connected with elastic spring is introduced, its calibration procedure is described, and the simulation of its response to force impulses with different duration is shown. Then a five-parametric variant of the reduced order model is presented, calibrated and tested. Combined with the Hertzian theory of non-adhesive contact, the model allows us to determine the time evolution of contact force for arbitrary mass, stiffness and initial velocity of the impactor. The simulated results are compared to experimentally obtained data and observations about the model properties and accuracy are made.
Keywords: dynamic analysis, force impulse, glass plate, Hertzian contact, impact loading, reduced order model.

1 INTRODUCTION

To properly account for damage evolution in glass plates caused by low-velocity impacts, it is necessary to evaluate the time evolution of contact force. This force obviously depends on velocity, stiffness and mass of the impactor but also on the dimensions of the glass plate, its material properties and supports. To simulate the phenomenon, it is essential to properly incorporate the dynamic forces acting on the impactor and the glass plate. The motion of the plate is often highly influenced by its supports because these may not be ideally stiff and/or may introduce significant damping. From this point of view, the experimental setup often avoids as much supports as possible especially in the direction of expected displacements. An advantageous setup that aims to eliminate the effect of imperfect supports consists of a vertically positioned glass plate freely hanging on suspension cables and being impacted horizontally to its center, see Fig. 1a. Such an idealized setup is assumed throughout this article. The experimental device is shown in Fig. 1b.
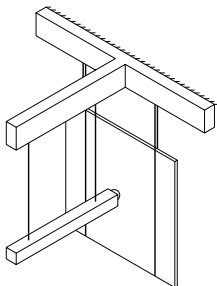
(a) Schema of impactor and glass plate   (b) Top view

Figure 1: Experimental setup of impactor and glass plate. The plate is unsupported in the direction of impact to minimize damping and other uncertainties attributed to imperfect supports.

2 REDUCED ORDER MODEL

When a force acts for a short time on its center, the unconstrained glass plate starts to accelerate. Due to the plate's flexibility, its center accelerates faster than its edges and the plate bends. Nevertheless, as the plate deforms, its edges start to accelerate too, and its center decelerates due to the internal forces. Thus the unconstrained plate starts to *translate* in the direction of the impact and also *oscillate* in its symmetric eigenmodes.

The simplest model able to describe such motion is an unconstrained system with two degrees of freedom consisting of two masses m_1 and m_2 and one spring with stiffness k as shown on the right-hand side of Fig. 3. This reduced order model for the plate is denoted here as the 2DoF model. Our goal is to determine these parameters so that the motion of mass m_1 corresponds to the motion of the center of the plate during and after the impact. The calibration procedure is based on three requirements:

1. The total mass of the 2DoF model has to be the same as the total mass of the plate, i.e.

$$m_1 + m_2 = m_{tot} \tag{1}$$

   where m_1 is mass of the impacted DoF, m_2 is mass of the other DoF and m_{tot} is the mass of the plate.

2. The eigenfrequency of the 2DoF model ω_{2DoF} has to be equal to the lowest eigenfrequency of the plate for which the eigenmode is non-zero at the center of the plate. This means that motion in this mode can be induced by force acting in the middle of the plate. Examining the first few eigenmodes in Fig. 2 suggests that this is, in fact, the third eigenfrequency but here denoted as ω_1. The requirement of equal eigenfrequencies is therefore written as

$$\omega_{2DoF} = \omega_1 \tag{2}$$

3. Finally, we require that the energies stored in the oscillating systems are equal. More specifically, when the mass m_1 oscillates with the same amplitude as the center of the plate, then the energy attributed to oscillations is the same in both models

$$U_{2DoF} = U_1 \tag{3}$$

Next section describes how to compute the eigenfrequencies of the plate and the corresponding energy attributed to the chosen eigenmode. These values are later utilized for model calibration.

2.1 Equations of motion and modal analysis of plate

The equations of motion for elastic body are written in weak form as

$$\int_\Omega \delta u \cdot \rho \ddot{u} \, d\Omega + \int_\Omega \nabla \delta u : \sigma \, d\Omega = \int_\Omega \delta u \cdot b \, d\Omega + \int_\Gamma \delta u \cdot t \, d\Gamma \tag{4}$$

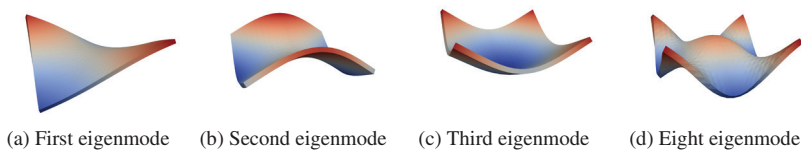(a) First eigenmode   (b) Second eigenmode   (c) Third eigenmode   (d) Eight eigenmode

Figure 2: Bending eigenmodes of unsupported rectangular plate.

where u is the field of displacements, $\ddot{u}$ the second derivative with respect to time t, i.e. the acceleration, ρ the material mass density, b the body forces and t the tractions on the body's boundary. The field δu is the virtual displacement vanishing on those parts of boundary where u is prescribed. The stress σ is given by

$$\sigma = \lambda \, t_r(\varepsilon)I + 2\mu\varepsilon \tag{5}$$

with the strain ε being the symmetric part of the displacement gradient

$$\varepsilon = \frac{1}{2}\left(\nabla^T u + \nabla u\right) \tag{6}$$

Discretizing the weak form gives a system of algebraic equations in the form

$$M\ddot{r} + Kr = F \tag{7}$$

where M is the mass matrix, K the stiffness matrix, r the vector of nodal displacements and F the vector of nodal load. Then the eigenfrequencies and eigenmodes result from $[-\omega^2 M + K]u = 0$. First six eigenfrequencies are equal to zero and correspond to rigid body modes. Let us denote ω_1 the first non-zero eigenfrequency with non-zero eigenmode at the center of the plate. The corresponding eigenmode is dented u_1. The potential energy attributed to oscillations in this eigenmode is

$$U_1 = \frac{1}{2}u_{1,n}^T K u_{1,n} \tag{8}$$

where the subscript n denotes normalized eigenmode with the deflection at the center equal to 1.

2.2 Modal analysis of 2DoF model

The equations of motion of the 2DoF system are

$$M\ddot{u}(t) + Ku(t) = \begin{bmatrix} m_1 & 0 \\ 0 & m_2 \end{bmatrix}\begin{Bmatrix} \ddot{u}_1(t) \\ \ddot{u}_2(t) \end{Bmatrix} + \begin{bmatrix} k & -k \\ -k & k \end{bmatrix}\begin{Bmatrix} u_1(t) \\ u_2(t) \end{Bmatrix} = \begin{Bmatrix} F_1(t) \\ 0 \end{Bmatrix} = F(t), \tag{9}$$

where m_1 and m_2 is the mass of the first and second degrees of freedom, respectively, symbol k denotes the stiffness of the spring, $F_1(t)$ the time-dependent force acting on the first mass and u_1 and u_2 the displacements of the two masses, see Fig. 3. The eigenfrequencies ω_i, $i = 0,\ldots,1$ of the 2DoF system solve the equation

$$\left[-\omega_i^2 M + K\right]u_i = 0 \tag{10}$$

where ω_i is the ith angular eigenfrequency and u_i is the corresponding eigenmode. For this particular system, $\omega_0 = 0$ corresponds to the rigid body mode and the frequency of the oscillations $\omega_{2DoF} = \omega_1$ depends on the model parameters according to

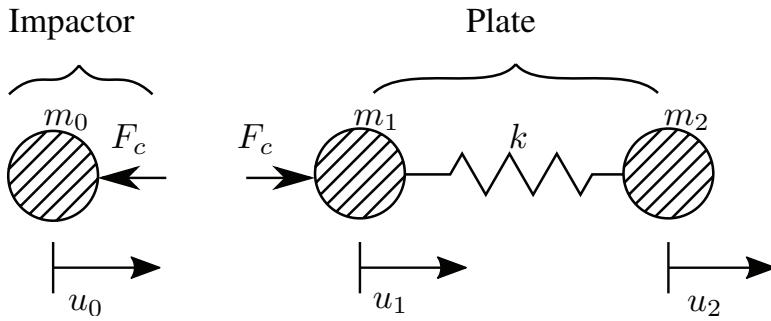$$\omega_{2DoF} = \sqrt{\frac{k(m_1 + m_2)}{m_1 m_2}}. \tag{11}$$

Figure 3: Schema of the 1DoF model for impactor and 2DoF model for plate.

By substituting the above expression into eqn (10), we obtain eigenmode $u = \{\xi/m_1, \xi/m_2\}^T$ for any real ξ. After normalizing the eigenmode such that the displacement of the first mass equals 1, we get $u = 1, m_1/m_2$. The elastic energy stored in the spring when the two masses are displaced according to the normalized eigenmode becomes

$$U_{2\text{DoF}} = \frac{1}{2}u^T K u = \frac{1}{2}k\left(1 + 2\frac{m_1}{m_2} + \frac{m_1^2}{m_2^2}\right).$$ (12)

2.3 Calibration

To recapitulate, we are searching for m_1, m_2 and k while knowing m, ω_1 and U_1 calculated for the plate. Let us express the masses of 2DoF model as

$$m_1 = \alpha m, \quad m_2 = (1 - \alpha)m$$ (13)

Next, expressing k from eqn (11), substituting it into eqn (12) and further substituting m_1 and m_2 from eqn (13) leads to

$$U_{2\text{DoF}} = \frac{1}{2}\frac{\alpha}{1-\alpha}\omega^2 m u_1^2$$ (14)

Rearranging the above equation gives

$$\alpha = \frac{2E}{2E + \omega^2 m u_1^2}$$ (15)

The distribution of mass between the two degrees of freedom now follows from eqn (13) and the stiffness from eqn (11).

2.4 Numerical tests of 2DoF model for plate

The response of the 2DoF model was compared to the response of an equivalent 3D finite element model. The FEM model of the plate was created in FEniCS package [1], discretized with quadratic tetrahedral elements and integrated over time using generalized α method [2]. Dimensions of the square plate are $0.5 \times 0.5 \times 0.015$ m, Young's modulus of glass is assumed

$E = 72.0 \times 10^9$ Pa, Poisson's ratio $v = 0.22$ and mass density $\rho = 2500$ kg/m3 corresponding to total mass $m = 9.375$ kg. The parameters of the 2DoF model are $m_1 = 2.378$ kg, $m_2 = 6.997$ kg and $k = 9.12 \times 10^6$ N/m. Responses to force impulses of 1 N with different duration are compared in Fig. 4. Figure 4a demonstrates high accuracy of the time evolution of displacement u_1 computed by the 2DoF model for relatively long force impulse. Note, that the acceleration during the force impulse is followed by linear motion with superposed harmonic oscillations. The match between predicted energies is also perfect, see Fig. 4b. Most of the energy added into the system transforms into kinetic energy attributed to the linear motion with only small fraction of the energy attributed to oscillations. This energy alternates between kinetic and potential depending on the current phase of the oscillations. Figures 4c and d show the evolution of displacements and energies during and after force impulse with shorter duration. In this case, the oscillatory part of the motion is more significant. The slight difference in total energy added to the system is caused by the fact that the simple 2DoF model does not vibrate

(a) Displacements due to force impuse 0.01s

(b) Energies due to force impulse 0.01s

(c) Displacements due to force impulse 0.001s

(d) Energies due to force impulse 0.001s

(e) Displacements due to force impulse 0.0002s

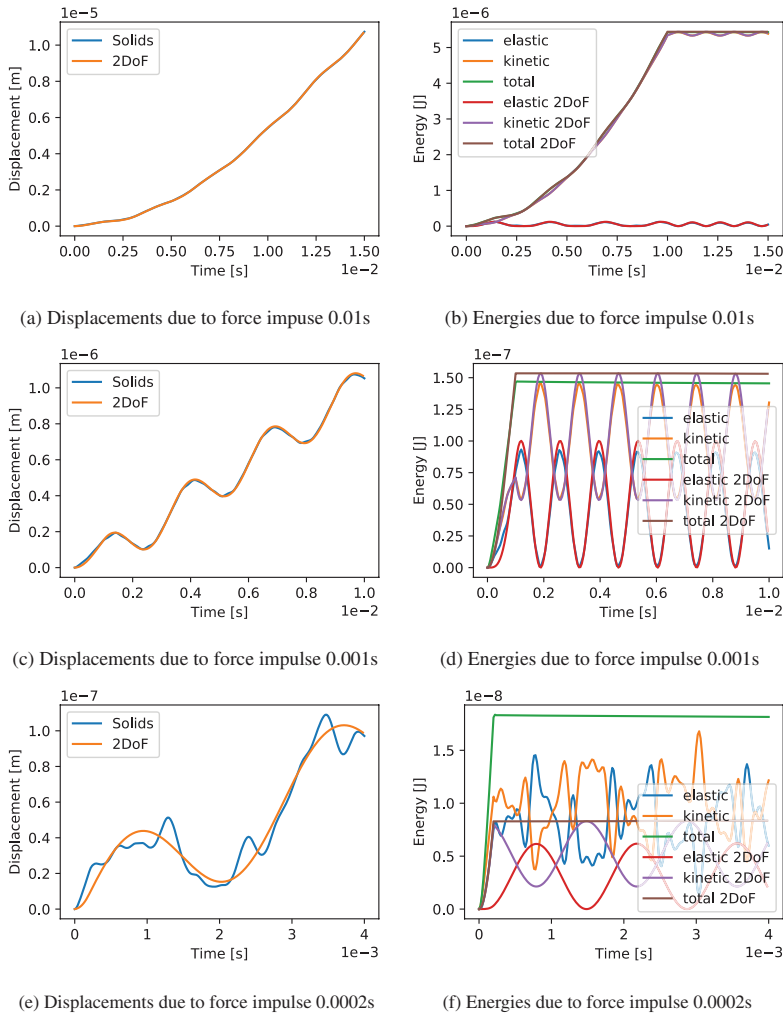(f) Energies due to force impulse 0.0002s

Figure 4: Comparison of 2DoF model and FEM model of glass plate.

on higher eigenfrequencies while the full 3D FEM model does. This phenomenon is even more visible for 0.2 ms impulse, see Figs. 4e and f, when the FEM model accumulates more than twice the energy accumulated by the 2DoF model. This is again attributed to strict kinematic restrictions enforced by the simple 2DoF model. This motivates the next section where one additional degree of freedom is added to the reduced order model to allow for oscillation in two eigenmodes.

2.5 3DoF model for plate

In this section, we add yet another degree or freedom to the model described in Section 2.2 so that the plate itself consists of three degrees of freedom with masses m_1, m_2 and m_3. The masses are connected with springs k_2 and k_3. We denote this version of the reduced order model for plate as the 3DoF model. Computing the values of its parameters follows rules analogous to rules in Section 2: (1) sum of masses equals the mass of the plate, $m_1 + m_2 + m_3 = m_{tot}$, (2) the two non-zero eigenfrequencies of the 3DoF model correspond to the first two eigenfrequencies of the plate that have non-zero eigenmode at center of the plate, i.e. vibration in these eigenmodes can be induced by impacting the center of the plate, see the eigenmodes in Figs. 2c and d for clarification, (3) oscillations in these normalized eigenmodes store same energies as corresponding oscillations of the plate. The motion of the 3DoF model is governed by system of three equations. Although the eigenfrequencies and the energies can be easily expressed in closed form, the same does not hold for parameters m_1, m_2, m_3, k_2 and k_3. Therefore, we cannot follow procedure in Section 2.2. Instead, the parameters were determined by minimization of objective function

$$f_{obj}(m_2, m_3, k_2, k_3) = R^T R \qquad (16)$$

where the vector of residua is written as

$$R = \left\{ \frac{\omega_1 - \bar{\omega}_1}{\bar{\omega}_1}, \frac{\omega_2 - \bar{\omega}_2}{\bar{\omega}_2}, \frac{U_1 - \bar{U}_1}{\bar{U}_1}, \frac{U_2 - \bar{U}_2}{\bar{U}_2} \right\}^T \qquad (17)$$

counterparts obtained by modal analysis of the plate. Thus calling function f_{obj} involves solving the eigenvalue problem of 3×3 matrix and computing the energies while assuming $m_1 = m_{tot} m_2 m_3$. The Nelder–Mead method implemented in `scipy.optimize` package was used to minimize the objective function and obtain the parameters of the 3DoF model.

2.6 Numerical tests of 3DoF model for plate

Analogically to Section 2.4, we present numerical tests in which the 3DoF model is subjected to force impulse and compare the results with the reference FEM solution. The model parameters were determined according the procedure described in Section 2.5, their values are $m_1 = 1.408 \, \text{kg}$, $m_2 = 1.578 \, \text{kg}$, $m_3 = 6.413 \, \text{kg}$, $k_2 = 2.523 \times 10^7 \, \text{N/m}$ and $k_3 = 1.164 \times 10^7 \, \text{N/m}$. Figure 5a shows just a slight improvement of the displacement evolution computed with the 3DoF model when compared to the 2DoF model in Fig. 4c. The slight difference of the displacements evolution during the period when the force impulse is applied might, however, qualitatively influence the system behavior during impact as shown in the following sections. For shorter impulse, the difference between the 3DoF model and the 2DoF model is even more visible, compare Figs. 5c and 4e. Even though the model is still stiffer than the reference FEM model and thus underestimates the energy absorbed by the system during force impulse, the error in total energies in Fig. 5d was substantially reduced.
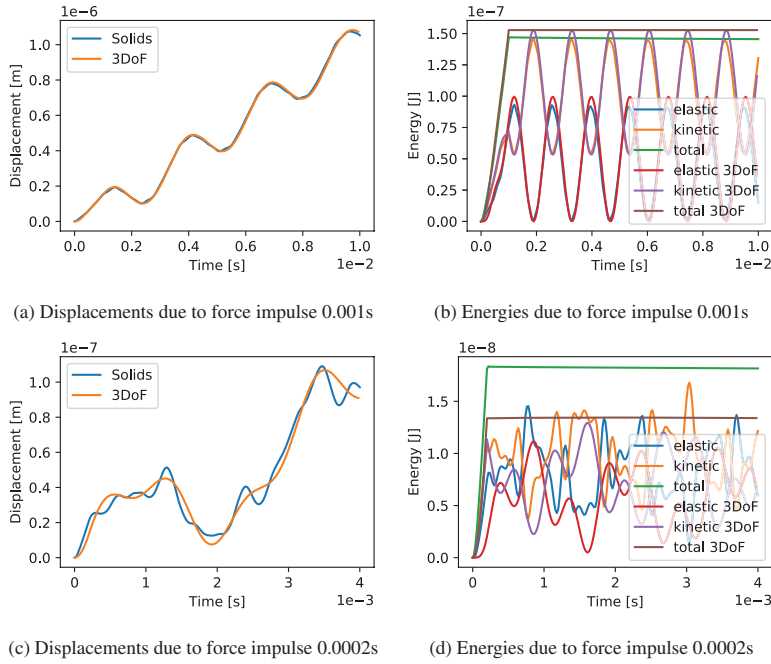
(a) Displacements due to force impulse 0.001s   (b) Energies due to force impulse 0.001s

(c) Displacements due to force impulse 0.0002s   (d) Energies due to force impulse 0.0002s

Figure 5: Comparison of the response of the 3DoF model to a force impulse with different duration with the response of the reference FEM model.

3 LOADING BY IMPACT

Closed form solutions exist for frictionless contact, see e.g. [3]. In particular, the force on the contact between spherical and flat surface is expressed as a function of penetration depth d of these two objects

$$F_c\left(d\right) = \begin{cases} \dfrac{4}{3} E * R^{\frac{1}{2}} d^{\frac{3}{2}} & \text{if } d > 0, \\ 0 & \text{otherwise.} \end{cases} \tag{18}$$

where R is the diameter of spherical surface that impacts the glass plate and the effective Young's modulus $E*$ is given by

$$E* = \frac{1}{\dfrac{1 - v_0^2}{E_0^2} + \dfrac{1 - v_1^2}{E_1^2}} \tag{19}$$

where E_1 and E_2 are Young's moduli of the two potentially different materials and v_1 and v_2 are Poisson's ratios. For negative penetration depth $d < 0$, the contact force is obviously zero. Writing equations of motion, i.e. the equilibrium conditions at any time, for each degree for freedom in the system in Fig. 3 gives us

$$m_0\ddot{u}_0 + F_c\left(u_0 - u_1\right) = 0 \tag{20}$$

$$m_1\ddot{u}_1 - F_c\left(u_0 - u_1\right) + k\left(u_1 - k_2\right) = 0 \tag{21}$$

$$m_2\ddot{u}_2 - k\left(u_1 - k_2\right) = 0 \tag{22}$$

Furthermore, we assume an unsupported glass plate loaded only by the impactor with known initial velocity $\dot{u}_0(t = 0) = v_{\mathrm{imp}}$. Such system can be easily integrated by suitable forward integration scheme, for example, the one implemented in `scipy.integrate.odeint`. The only remaining technicality is to convert the system of second-order differential equations into standard form $\dot{y} = F(y,t)$. This is done by defining velocities $v_i = \dot{u}_i$ and using them to get rid of the second derivatives of displacement. Now the system becomes

$$\dot{v}_0 = -\frac{F_c\left(d = u_0 - u_1\right)}{m_0} \tag{23}$$

$$\dot{v}_1 = \frac{F_c\left(d = u_0 - u_1\right) - k\left(u_1 - u_2\right)}{m_1} \tag{24}$$

$$\dot{v}_2 = \frac{k\left(u_1 - u_2\right)}{m_2} \tag{25}$$

$$\dot{u}_0 = v_0 \tag{26}$$

$$\dot{u}_1 = v_1 \tag{27}$$

$$\dot{u}_2 = v_2 \tag{28}$$

The initial condition for such system is $v_0(t = 0) = v_{\mathrm{imp}}$ and the initial values of the remaining components are zero.

3.1 Numerical tests of model for impactor and plate

In this section, we assume either 2DoF or 3DoF model for plate with the parameters presented in Sections 2.4 and 2.6. The model presented in previous section assumes the impactor being stiff and its motion being described by a single degree of freedom. Nevertheless, the finite stiffness of the impactor is taken into account in equn (18). Parameters $E_0 = 210 \times 10^9$ Pa, $v_0 = 0.3$, $m_0 = 52$ kg, $R = 0.05$ m and $v_{0,\mathrm{in}} = 0.4429$ m/s were assumed for the impactor. Figure 6a compares the displacement of the impactor u_0 and the displacement of the center of glass plate u_1 between 2DoF and 3DoF models. At time $t = 0$ s, the impactor touches the glass and the spherical head starts to penetrate the glass surface. A series of several such contacts accelerated the plate so it finally departs the impactor and moves faster in linear motion. Slight oscillations are being superposed onto the linear motion. A detail of this data in the period of the impact is displayed in Fig. 6b. Note that the moments when the u_1 line is below the u_0 line correspond to positive penetration depth and thus presence of contact force F_c. Figures 6c and

(a) Displacement of the impactor and the center of the galas plate

(b) Detail of displacement during impact

(c) Velocity of the impactor and the center of the galas plate
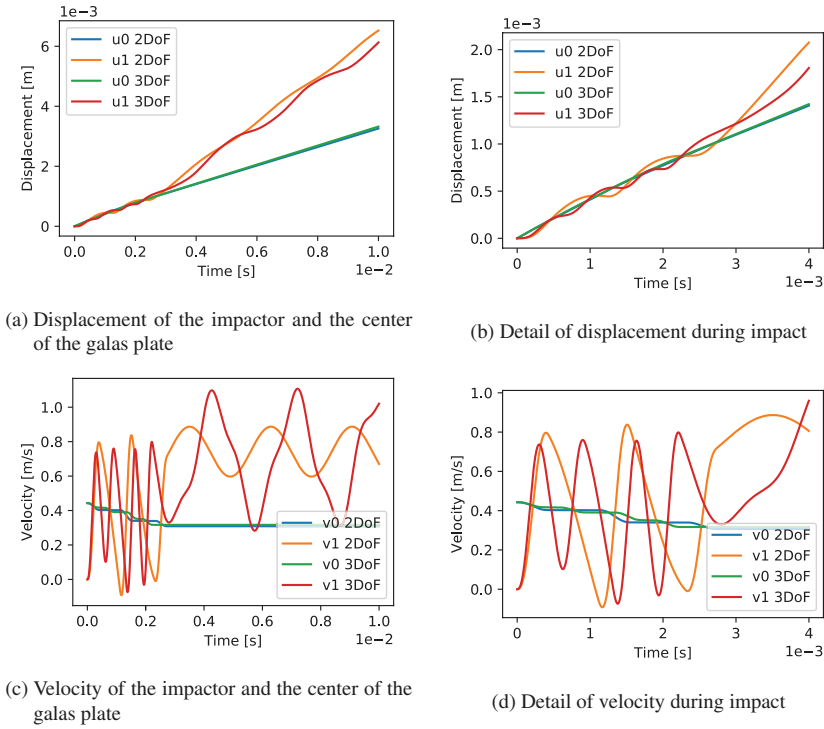

(d) Detail of velocity during impact

Figure 6: Simulation of impact using 2DoF and 3DoF model for glass plate.

d show the evolution of velocities. It can be observed again that the glass starts at rest and is accelerated by series of short contacts impactor. The impactor on the other hand decelerates slightly but still moves in its original direction with lower velocity than the glass plate.

3.2 Comparison with measured data

The presented two variants of the reduced order model were compared wviith results of the preliminary non-destructive test performed at the Experimental Center of the Faculty of Civil Engineering, Czech Technical University in Prague. A plate made of float glass positioned according to the schema in Fig. 1a was repeatedly impacted by an impactor with steel spherical head. The acceleration of the impactor and several points on the glass surface were measured by accelerometers. The motion during and after the impact was also recorded by high-speed camera in order to compute the displacement field by means of digital image correlation. At the time of writing, only the data from the accelerometers were available. For both, the reduced order models and the experimental data, the contact force was computed from the acceleration of the impactor according to

$$F_c(t) = -m_0 \ddot{u}_0(t) \tag{29}$$

The measured acceleration was stripped of noise using CFC600 filter [4]. The filter is a standardized Butterworth low pass filter commonly applied to acceleration signals obtained during impact measurements. The evolution of contact force computed with the 2DoF and

(a) Computed contact force compared to the values obtained experimentally from measured impactor accelerations
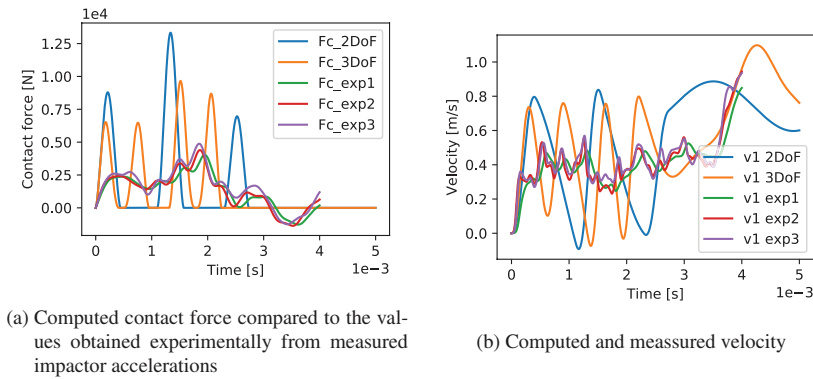
(b) Computed and meassured velocity

Figure 7: Computed contact force and velocity of the center of the plate compared to the experimentally obtained values.

3DoF models for the plate is compared in Fig. 7a to three series of experimentally obtained values. It can be observed that both models predict several consecutive contacts between the glass plate and the impactor. On the other hand, the measured accelerations suggest that the impactor is in contact with the glass plate during the entire duration of impact. Nevertheless, it is not clear to what extent is this observation influenced by the applied filter. The total duration of the impulse is predicted quite accurately by both models. On the other hand, this does not hold for force magnitude which is about two times overestimated for 3DoF model and even more for 2D of model.

Figure 7b compares the computed velocities of the plate center point to the measured values. The measured values of velocity were obtained by integrating the filtered acceleration signals. Again, the predicted velocity during the impact fluctuates more than the observed data but the moment at which the glass detaches from the impactor and the subsequent velocity evolution is predicted accurately.

4 CONCLUSIONS

Two variants of very simple reduced order model for unsupported glass plate exposed to low-velocity impact were described. The 2DoF resp. 3DoF model is calibrated to mimic the oscillation of the plate in one resp. two chosen eigenfrequencies. The simple 2DoF variant of the model requires just three model parameters. The calibration procedure is based on the equivalence of energies stored in the oscillating systems and written in closed form. Calibration of the 3DoF model with five parameters is based on identical principles, but the parameters were obtained by minimization of an objective function. Numerical tests show that both models accurately simulate the response to longer force impulse. Simulations of a very short force impulse are less accurate because such impulse activates higher harmonic frequencies which these models, with just two or three degrees of freedom, cannot cover.

Modeling of impact is governed by Hertzian Law for frictionless contact between the elastic spherical surface and flat surface. This law is written in simple power law and relates the contact force to the penetration depth while accounting for the elastic parameters of the two materials and radius of the spherical surface.

The models were calibrated for 0.5×0.5 m glass plate 15 mm thick to simulate its behavior during a low-velocity impact. Accelerometers attached to the impactor and the glass plate monitored the acceleration during tests. These signals were used to express the evolution of

the contact force and the velocity of the center point on glass plate. Comparison of the computed values to the measured ones not only validates the model but also shows its limitations. The main drawback is higher stiffness of both reduced order models given by the fact that their motion is limited only to one or two eigenmodes. On the other hand, the duration of the impact and the subsequent velocity of the plate is predicted quite accurately. Given what we have learned, the presented reduced order model would be more accurate for modeling impact between softer bodies which are in contact for a longer period than stiff objects. On the other hand, using the model to evaluate the loading effect caused by mid- to high-velocity impact of relatively hard bodies would significantly overestimate the peak value of the contact force.

REFERENCES
[1] Logg, A., Mardal, K.A. & Wells, G.N. (eds), *Automated Solution of Differential Equations by the Finite Element Method: The FEniCS Book*, Vol. 84, Springer, 2012.
[2] Chung, J. & Hubert, G.M., A time integration algorithm for structural dynamics with improved numerical dissipation: The generalized-α method. *ASME Journal of Applied Mechanics*, **60(2)**, pp. 371–375, 1993. https://doi.org/10.1115/1.2900803
[3] Johnson, K.L., *Contact Mechanics*, Cambridge University Press, 1985.
[4] Covaciu, D. & Dima, D.S., Crash tests data acquisition and processing. In *CONAT 2016 International Congress of Automotive and Transport Engineering*, pp. 782–789, 2017.